DOI 10.5012/bkcs.2011.32.1.186

Synthesis of Ordered Mesoporous Manganese Oxides by Double Replication for Use as an Electrode Material

Xiao-Feng Guo and Geon-Joong Kim*

*Department of Chemical Engineering, Inha University, Incheon 402-751, Korea. *E-mail: kimgj@inha.ac.kr*
Received September 6, 2010, Accepted November 10, 2010

Periodically ordered mesoporous manganese oxides were synthesized in a single and double replication procedure. Mesoporous SBA-15 and -16 silica and their reverse replica carbons were successively used as hard templates. The silica and carbon pore systems were infiltrated with $Mn(NO_3)_2{\cdot}xH_2O$ or $Mn(AcAc)_2$, which was then converted to Mn_2O_3 at 873 K; the silica and carbon matrix were finally removed by NaOH solution or calcinations in air. The structure of the mesoporous Mn_2O_3, using a carbon template, corresponds to that of the original SBA-15 and SBA-16 silica. The products consist of hexagonally arranged cylindrical mesopores with crystalline pore walls or cubic mesoporous pores. The structure of replica has been confirmed by XRD, TEM analysis, and its electrochemical properties were tested with cyclic voltammetry. Formation of Mn_2O_3 inside the mesoporous carbon pore system showed much improved electrical properties.

Key Words: Mesoporous Mn_2O_3, Reversible replication, Cyclic voltammetry, Chemical vapour deposition, Nanomaterials

Introduction

The synthesis of organized mesoporous materials has stimulated extensive research over the past decade.[1-6] In particular, mesoporous materials with a transition-metal oxide framework have immense potential for applications in catalysis, photocatalysis, sensors, and electrode materials because of their characteristic catalytic, optical, and electronic properties.

However, for select applications, this potential can only be maximized in the highly crystalline state. High thermal and mechanical stabilities are also associated with the crystalline state. Despite many efforts, up until today, it remains a major challenge to successfully convert the amorphous walls of as-made materials to crystalline walls during the crystallization process, while simultaneously retaining the original mesostructure. This is often the case as heat treating the material at higher temperatures results in changes to the crystal structure of the oxide and subsequent loss of the mesostructure.

Mesoporous manganese oxides with an ordered mesoporous structure, large specific surface area, and crystalline walls are expected to provide enhanced electrical performance due to their large specific surface area. In addition, they are also potentially useful as electrode materials in lithium-ion batteries, as their regular porosity would permit intimate flooding of the electrolyte within the particles, and their crystalline walls could be important in promoting lithium intercalation.[7] However, to the best of the authors' knowledge, no original ordered mesoporous manganese oxides have been synthesized using carbon matrixes. Herein, we describe the first synthesis of mesoporous manganese oxides with a periodically ordered uniform pore system, narrow pore-size distribution, and crystalline walls using mesoporous carbons as hard templates.

Experimental

Synthesis of Mesoporous Manganese Oxides by a Carbon Template. Silica and carbon templates were synthesized using modified literature procedures.[8-10] The following wet impregnation procedure was used for synthesis of mesoporous Mn_2O_3, unless otherwise noted: A 1.0 g sample of CMK-3 or C-SBA-16 was dispersed in 2.0 mL of a tetrahydrofuran (THF) solution (1.0 mol L^{-1}) of $Mn(OAc)_2$ (Aldrich) and the resulting solution stirred for 2 h to impregnate $Mn(OAc)_2$ in the mesopores of carbon template. After filtration and drying, the sample was heated under an air atmosphere to 573 K at a constant rate of 2.5 K min^{-1} to convert the $Mn(OAc)_2$ to manganese oxide. This procedure was repeated twice. Crystalline products were obtained by keeping the sample at 573 K for 3 h. The carbon was removed by heating the sample under an air atmosphere at 873 K at a constant rate of 2.5 K min^{-1} and keeping the sample at that temperature for 2 h. The samples were designated as Mn_2O_3-CMK-3 and Mn_2O_3-C-SBA-16, respectively.

Synthesis of Mesoporous Manganese Oxides by a Silica Template. A general route for synthesis is as follows: 0.8 g of manganese nitrite ($Mn(NO_3)_2{\cdot}xH_2O$) aqueous solution (50%) was mixed with 0.15 g of SBA-15 or SBA-16 in 6.5 mL ethanol with stirring for 2 h. The solid sample was collected after evaporation of ethanol and water solvent, and then heated from room temperature to 873 K (forming Mn_2O_3) at a heating rate of 2.5 K min^{-1}, and maintained at the final temperature for 5 h. The products (Mn_2O_3) were immersed in hot NaOH at 353 K to remove the silica template, recovered by centrifugation, and washed with distilled water three times. The obtained manganese oxides will be designated as Mn_2O_3-SBA-15 and Mn_2O_3-SBA-16. The procedures to obtain the different type of mesoporous Mn_2O_3 are represented in Scheme 1.

The optimum conditions for a successful infiltration of the mesopores are dependant mainly on the polarity of pore surfaces. Because the mesoporous silica possesses different wetting properties from the carbon due to the high hydrophilicity of surfaces, the source of manganese was varied properly with different solvent system, as mentioned above: the choice of solvents should be a compromise between the adequate wettability of pore surfaces and the high solubility of metal salt.

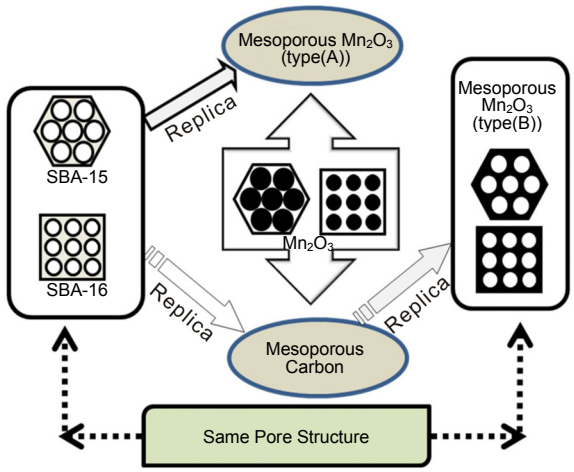

Scheme 1. Schematic illustration for the synthesis of mesoporous Mn_2O_3 using mesoporous silica and carbon as templates.

Characterization. X-ray powder diffraction (XRD) data were acquired on a D/MAX 2500V/PC diffractometer using Cu Kα radiation. The morphology and microstructures of as-prepared samples were characterized by field emission transmission electron microscopy (FE-TEM, S-4200). The nitrogen adsorption/desorption analysis was performed at −196 °C by using a BET surface area and porosity analyzer equipment (Micromeritics, ASAP 2010). Electrochemical properties of mesoporous metal oxides were tested with cyclic voltammetry (CV; Autolab 128N).

Results and Discussion

Figure 1 shows the powder X-ray diffraction diagram of SBA-15 and SBA-16 silica, mesoporous Mn_2O_3 replicas using silica and carbon as their templates, respectively: The mesoporous Mn_2O_3-CMK-3 was prepared by twice reversible replication of SBA-15 to show a near identical XRD pattern with starting SBA-15 template. This indicated that the structure of Mn_2O_3-CMK-3 returned back to the silica matrix (SBA-15). Low-angle reflections, corresponding to the two-dimensional hexagonal periodicity of the pore systems (P6mm), were visible in two samples (SBA-15 and Mn_2O_3-CMK-3). However, the first replication step (SBA-15 to Mn_2O_3-SBA-15) entailed slight shrinkage of the periodic distance, indicated by a shift of the reflections toward wider diffraction angles; this is frequently observed in this type of silica-to-carbon replication. However, no significant further changes in the reflection angles were observed in the second replication step (SBA-15-CMK-3 to Mn_2O_3-CMK-3): the resultant Mn_2O_3-CMK-3 can be considered the positive replica of SBA-15 silica (and as the negative replica of CMK-3 carbon), although a certain degree of broadening and poorer resolution of the reflections indicate some loss in structural order. Mn_2O_3-SBA-15 could be taken as the negative replica of SBA-15. The first and second replicas of SBA-16 were similar to SBA-15. The XRD pattern of SBA-16 and its replica (Mn_2O_3-C-SBA-16 and Mn_2O_3-SBA-16) showed well-resolved peaks at 2θ angles below 5°, which corresponded to the cubic im3m space group.

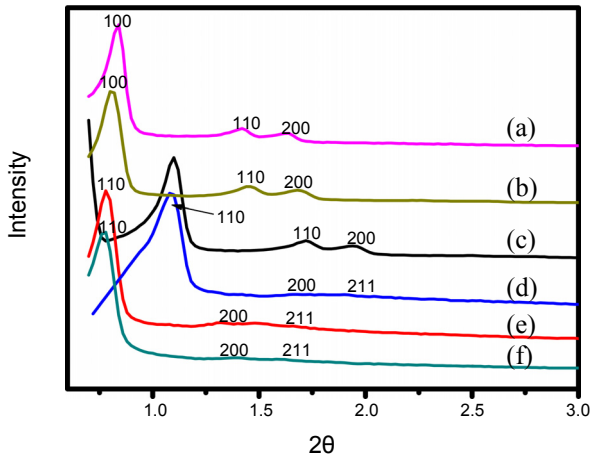

Figure 1. Low angle powder X-ray diffraction of: (a) SAB-15; (b) Mn_2O_3-CMK-3; (c) Mn_2O_3-SBA-15; (d) Mn_2O_3-SBA-16; (e) Mn_2O_3-C-SBA-16; (f) SBA-16.

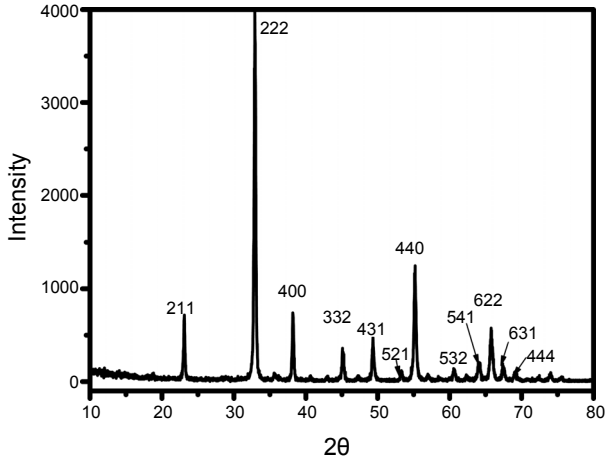

Figure 2. Highly ordered powder X-ray diffraction of Mn_2O_3-CMK-3.

The wide-angle powder X-ray diffraction diagram of mesoporous Mn_2O_3 (Fig. 2, inset) exhibited reflections attributable to the crystalline (rock salt) structure of manganese oxide; such crystallinity was observed when the samples were kept at 873 K for 5 h after conversion of $Mn(NO_3)_2{\cdot}xH_2O$ or $Mn(AcAc)_2$ to Mn_2O_3 within the silica or carbon matrix.

To confirm that the crystallinity exists in the mesoporous samples rather than in potential nonporous byproducts. TEM combined with SAED were carried out. Mn_2O_3-SBA-15 (Fig. 3(d) and 3(e)) showed a typical TEM images of SBA-15 templated porous crystals. The morphologies of these particles are same array of nanorods connected to each other by some small bridges. TEM images with higher magnifications of porous Mn_2O_3 crystal template by SBA-16 (Fig. 3(f)) indicated that porous crystals were both made of nanoballs connected by nanobridges in the SBA-16 templated Mn_2O_3, the nanospheres are in a body central arrangement. Mn_2O_3-C-SBA-16 which template from C-SBA-16 (Fig. 3(i)) showed a typical a space group im3m cubic structure as same as SBA-16 after twice replications.

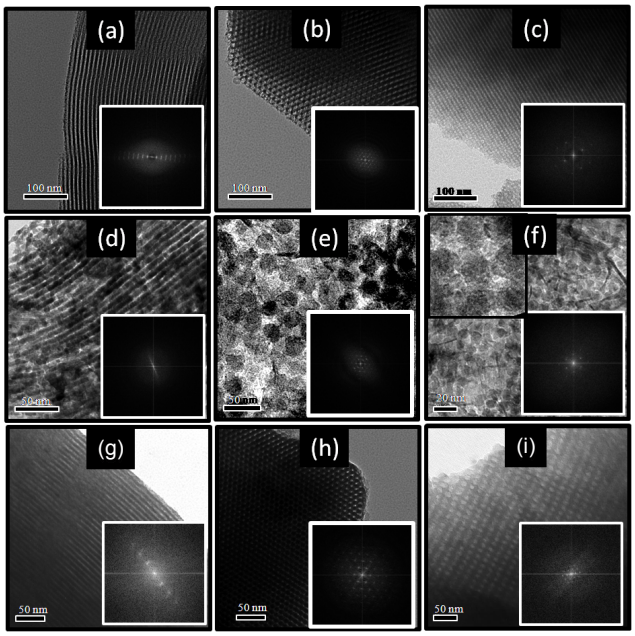

Figure 3. TEM images of: (a) SAB-15 [001]; (b) SBA-15 [110]; (c) SBA-16 [100]; (d) Mn_2O_3-SBA-15 [001]; (e) Mn_2O_3-SBA-15 [110]; (f) Mn_2O_3-SBA-16 [100]; (g) Mn_2O_3-CMk3 [001]; (h) Mn_2O_3-CMK-3 [110]; (i) Mn_2O_3-C-SBA-16 [100].

Table 1. Textural property of mesoporous silica and their replica (Mn_2O_3)

Sample	Surface area[a] (m^2 g^{-1})	Pore diameter[b] (nm)	Pore volume[b] (cm^3 g^{-1})
SBA-15	880	7.9	1.12
Mn_2O_3-SBA-15	102	2.7	0.23
Mn_2O_3-CMK-3	320	5.6	0.46
SBA-16	987	3.6	0.57
Mn_2O_3-SBA-16	113	2.3	0.28
Mn_2O_3-C-SBA-16	278	3.2	0.44

[a]Calculated by the BET method. [b]Calculated by the BJH method from desorption.

The nitrogen adsorption/desorption isotherms were determined to elucidate the pore structure of porous Mn_2O_3 replicated by different templates. The N_2 adsorption/desorption isotherms (type IV) of Mn_2O_3 templated by SBA-15 and CMK-3 confirmed the mesoporous properties with a specific surface area of 102 and 302 m^2/g, respectively. The pore structure of Mn_2O_3 templated by CMK-3 (Fig. 4(c)) was similar to SBA-15 and consistent with the XRD data, indicating that mesoporous Mn_2O_3-CMK-3, after twice reversible replication of SBA-15, would return back to the parent template (SBA-15). The N_2 adsorption/desorption isotherms (type IV) of Mn_2O_3 templated by SBA-16 and C-SBA-16 gave specific surface areas of 113 and 278 m^2/g, with pore volumes of 0.28 and 0.44 cm^3/g (Fig. 5(b) and 5(c)).

The CVs obtained with the bulk and porous Mn_2O_3 in 0.5 M Et_4NBF_4/propylene carbonate (PC) are shown in Fig. 6. The electrode displays a capacitive charging current in both (anodic

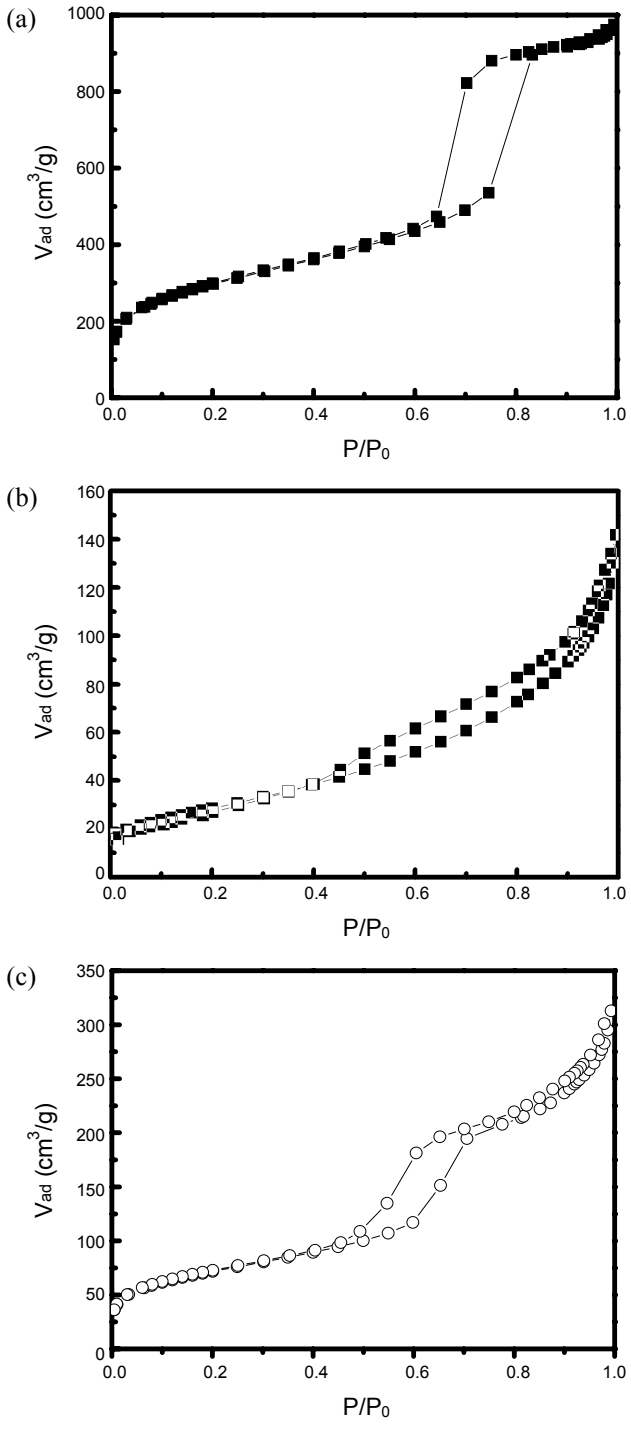

Figure 4. Nitrogen adsorption/desorption isotherms of: (a) SAB-15; (b) Mn_2O_3-SBA-15; (c) Mn_2O_3-CMK-3.

and cathodic) scanning directions across a potential range of −2.0 V to 2.0 V (*versus* Ag/AgCl reference electrode), and at a scan rate of 70 mV/s. As shown in Fig. 6, the redox current intensity of porous Mn_2O_3 crystal was much higher than its corresponding bulk. Mesoporous Mn_2O_3-CMK-3 showed the best redox current intensity. This can be interpreted in terms of the material's large surface area and highly ordered porous crystalline structure, which can provide fast and reversible

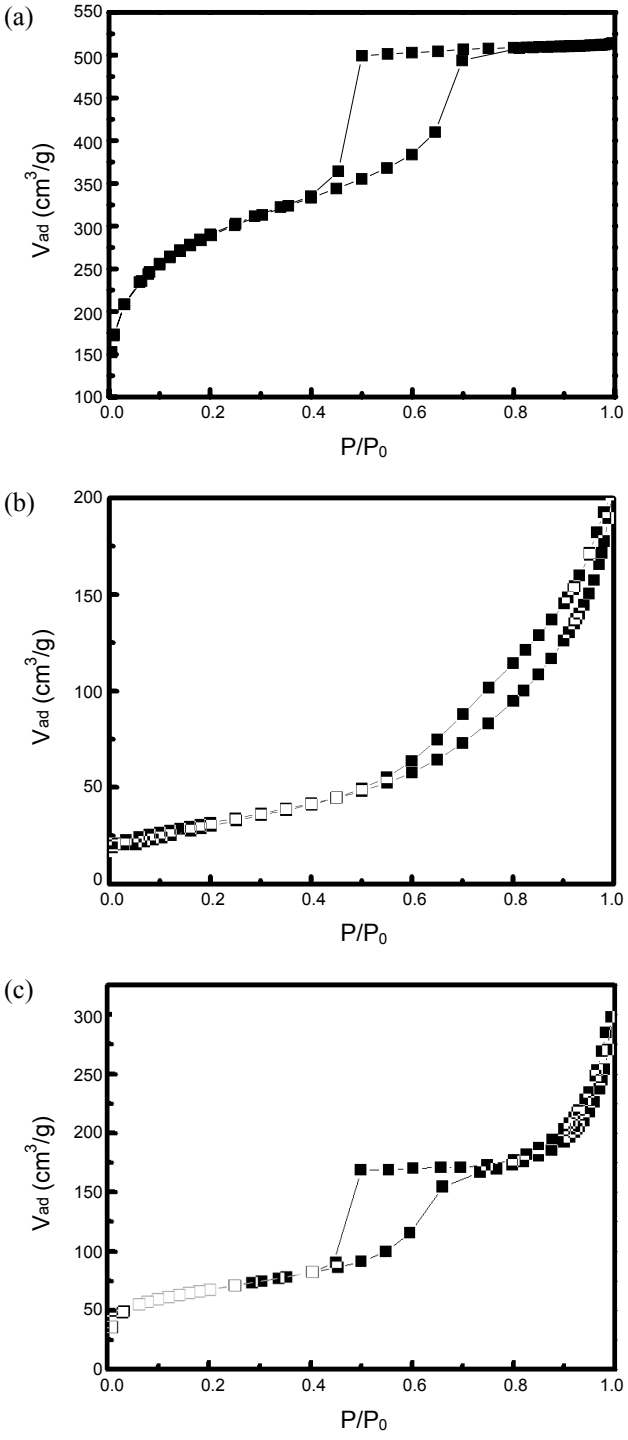

Figure 5. Nitrogen adsorption/desorption isotherms of: (a) SAB-16; (b) Mn_2O_3-SBA-16; (c) Mn_2O_3-C-SBA-16.

faradic reactions. Furthermore, the crystalline structures of Mn_2O_3 porous crystals have already been proven by TEM and XRD analysis.

In order to obtain more information on the electrochemical behavior of the synthesized porous Mn_2O_3 crystal template with the CMK-3 template, characterization of Mn_2O_3-CMK-3 was performed at different scan rates starting from 30 to 150 mV/s, and the results shown in Fig. 7. This will lead to a better understanding of the actual participation of the porous crystal electrodes in the redox process.

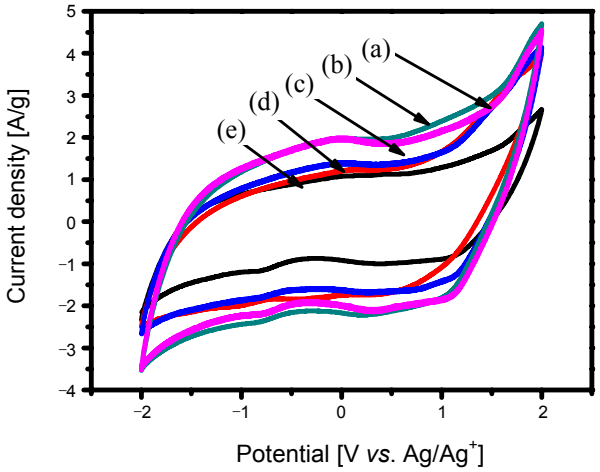

Figure 6. Cyclic voltamogram of: (a) Mn_2O_3-C-SBA-16; (b) Mn_2O_3-CMK-3; (c) Mn_2O_3-SBA-15; (d) Mn_2O_3-SBA-16; (e) bulk Mn_2O_3.

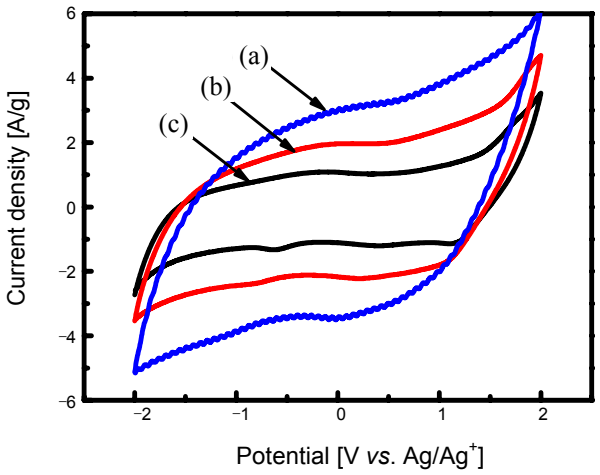

Figure 7. Cyclic voltamogram of Mn_2O_3-CMK-3 at different scan rates in 0.5 M Et_4NBF_4/propylene carbonate (PC): (a) 150 mV/s; (b) 70 mV/s; (c) 30 mV/s.

Conclusions

A novel mesoporous manganese oxide with a highly ordered 2D hexagonal or 3D cubic structure has been synthesized using mesoporous silica or carbon as templates. High current densities were obtained from porous Mn_2O_3 crystal templated by mesoporous carbon (CMK-3 and C-SBA-16). Such materials have big potentials in applications as lithium ion batteries, super capacitors, and semiconductors. Moreover, this study herein confirms that the "one step-further" nanocasting method can be extended to ordered mesoporous transition-metal oxide materials. Therefore, it is foreseeable that increasing numbers of mesoporous transition-metal oxide materials with various mesoporous structures would be synthesized with a similar method using mesoporous carbons with different pore connectivities and sizes.

Acknowledgments. This research was supported by Research grant of Inha University in 2010.

References

1. Ying, J. Y.; Mehnert, C. P.; Wong, M. S. *Angew. Chem. Int. Edn.* **1999**, *38*, 56.
2. Schüth, F.; Schmidt, W. *Adv. Mater.* **2002**, *14*, 629.
3. Kresge, C. T.; Leonowicz, M. E.; Roth, W. J.; Vartuli, J. C.; Beck, J. S. *Nature* **1992**, *359*, 710.
4. Asefa, T.; MacLachan, M. J.; Coombs, N.; Ozin, G. A. *Nature* **1999**, *402*, 867.
5. Garcia, C.; Zhang, Y. M.; DiSalvo, F.; Wiesner, U. *Angew. Chem. Int. Edn.* **2003**, *42*, 1526.
6. Mokaya, R. *Angew. Chem. Int. Edn.* **1999**, *38*, 2930.
7. Armstrong, A. R.; Paterson, A. J.; Robertson, A. D.; Bruce, P. G. *Chem. Mater.* **2002**, *14*, 710.
8. Zhao, D.; Feng, J.; Huo, Q.; Melosh, N.; Fredrickson, G. H.; Chmelka, B. F.; Stucky, G. D. *Science* **1998**, *279*, 548.
9. Jun, S.; Joo, S. H.; Ryoo, R.; Kruk, M.; Jaroniec, M.; Liu, Z.; Ohsuna, T.; Terasaki, O. *J. Am. Chem. Soc.* **2000**, *122*, 10712.
10. Kim, T. W.; Ryoo, R.; Gierszal, K. P.; Jaroniec, M.; Solovyov, L. A.; Sakamotod, Y.; Terasakid, O. *J. Mater. Chem.* **2005**, *15*, 1560.